The effect of photo-oxidation on the sticking and reactivity of Ag on amorphous GeS$_2$

The effect of photo-oxidation on the sticking and reactivity of Ag on amorphous GeS$_2$

J Hugh Horton†, Christopher Hardacre‡, Christopher J Baddeley, Geoffrey D Moggridge§, R Mark Ormerod‖ and Richard M Lambert¶

Department of Chemistry, University of Cambridge, Cambridge CB2 1EW, UK

Abstract. Photo-oxidation of amorphous GeS$_2$ films illuminated by band-gap radiation drastically alters the growth mode and reactivity of subsequently deposited Ag. In the former case (monolayer/simultaneous multilayer growth) the Ag reacts with both Ge and S sites. In the latter case (Stranski–Krastanov growth) Ge sites are selectively oxidized and film growth proceeds by Ag nucleation at the unoxidized S sites. The behaviour is very different from that reported earlier for Zn deposition on GeS$_2$, where photo-oxidation results in very large changes in metal sticking probability. XPS, XAES and EXAFS data provide the basis for understanding both this phenomenon and the very different photodiffusion behaviour of Zn and Ag in GeS$_2$.

1. Introduction

Chalcogenide vitreous semiconductors (ChVS) such as GeS$_2$ undergo an interesting photodiffusion reaction [1]. When a metallic layer (typically Ag or Zn) is deposited on a thin ChVS film ~100–1000 Å thick, illumination with band-gap light results in dissolution of the metal into the ChVS forming a metal-doped ChVS compound. In this reaction the metal–ChVS interface plays an important part in determining the transport behaviour [2], but very little is known about the structure and composition of this interface. For example, the induction period that precedes the onset of photodiffusion is very dependent on the method of ChVS and metal film preparation. This induction period has been ascribed to either oxidation of the semiconductor film or to formation of a metal–chalcogen compound at the interface [1]. It is also known that irradiation of various ChVS in the presence of band-gap light (photo-oxidation) can lead to very large decreases in the sticking probability of Zn or Cd metal on the ChVS surface during subsequent metal deposition [3]. This suggests that preferential oxidation of the non-chalcogen sites (i.e. Ge in the present case) is responsible for this phenomenon, and our recent work [4] has provided direct confirmation of this view. Very strikingly, the sticking probability of Ag on GeS$_2$ and other ChVS shows no such dependence on photo-oxidation of the semiconductor. The present paper addresses this question.

† Also at: Department of Chemistry, University of Western Ontario, London, Ontario, Canada N6A 5B7.
‡ Also at: Department of Chemistry, Queen's University, Belfast BT9 5AG, UK.
§ Also at: Department of Chemical Engineering, Cambridge University, Cambridge CB2 3RA, UK.
‖ Also at: Department of Chemistry, Keele University, Keele ST5 5BG, UK.
¶ Author to whom any correspondence should be addressed.

We have shown that it is possible to grow and characterize clean GeS$_2$ films under UHV conditions. By means of Auger spectroscopy we have also shown that photo-oxidation switches the growth mode of Ag on such GeS$_2$ films from monolayer/simultaneous multilayer to Stranski–Krastanov [5]. Here we report on an the application of XPS to characterize the electronic properties of the Ag/GeS$_2$ interface. Additionally, we have exploited the findings of our earlier work [5, 6] in order to prepare layered Ag/GeS$_2$ samples under UHV conditions: these have been used to examine structural aspects of the clean and photo-oxidized metal/semiconductor interface using EXAFS. We have characterized the extent of Ag–S versus Ag–Ge bonding on both the clean and the photo-oxidized films, and the results provide a basis for understanding the metal sticking probability phenomenon. In particular the large differences in behaviour exhibited by Ag on the one hand and Zn and Cd on the other may be explained. We also consider the characteristics of the interface in comparison with those predicted by models [1, 2] for the photodiffusion reaction and for the induction period effect.

2. Experimental details

Experiments were carried out in two UHV chambers which have been previously described [5, 7]. Both operated at base pressures of 1×10^{-10} Torr or better and were equipped with a pressure cell/transfer systems for preparation of the photo-oxidized GeS$_2$ films; in chamber A the pressure cell could also be used as an airlock. Chamber A was equipped with an RFA for AES measurements, an ion gun for Ar$^+$ cleaning and a quadrupole mass spectrometer for residual gas analysis. Chamber B was similarly equipped and included a VSW HA100 XPS/AES system. Al Kα radiation was used for acquiring XP spectra which were referenced to the valence band cut-off, and to the Ni 2p$_{3/2}$ peak (632.9 eV) from the Ni substrate. Both chambers were equipped with collimated GeS$_2$ and Ag evaporation sources whose operation and deposition characteristics have been described elsewhere [5, 6]. The GeS$_2$ films required for Ag deposition experiments were grown on Ni foil. These films were about 80 Å thick and have been characterized in some detail [5]. Photo-oxidation of the films was carried out in the pressure cell at O$_2$ pressures of 0.2 bar using a 1000 W Xe arc lamp. The preparation methods and characteristics of the photo-oxidized films have also been described previously [6]. The films used here were subjected to saturation photo-oxidation; under these conditions several monolayers of oxide formed on the surface.

The layered Ag/GeS$_2$ samples for use in the EXAFS experiments were prepared in chamber A under UHV conditions. Two samples were prepared without and with photo-oxidation of the ChVS; these will be referred to as sample 1 (Ag/GeS$_2$) and sample 2 (Ag/ox-GeS$_2$) respectively. Calibration of the deposited layer thicknesses of both GeS$_2$ and Ag was carried out using AES and by reference to our earlier work [5, 6]. The series of deposition stages for sample 1 was as follows:

(1) GeS$_2$ was deposited on the Ni foil substrate for 1 h (approximately 40 Å);
(2) Ag was deposited for 1 h (approximately 10 Å);
(3) GeS$_2$ was deposited for 20 min (approximately 12 Å);
(steps 2 and 3 were repeated a total of six times)
(4) GeS$_2$ was deposited for 1 h (approximately 40 Å).

The net result was a layered specimen which contained 12 Ag/GeS$_2$ interfaces. Sample 2 was prepared in the same manner, except that before each metal deposition stage, the GeS$_2$ layer was exposed to 0.2 bar of O$_2$ for 1 h and there was sufficient uv illumination in the pressure cell to photo-oxidize it to the saturation point. Once a sample was completed,

it was transferred out of chamber A using the airlock and placed in a desiccator where it was shielded from ambient light during storage and transfer to the synchrotron. EXAFS experiments were carried out on the Ge and Ag K edges at station 9.3, Daresbury Laboratory. Data were acquired in the fluorescence mode under ambient conditions. Several standard samples were also run: (i) an 80 Å GeS$_2$ film, also deposited under UHV conditions on a Ni foil, and examined in the fluorescence mode at the Ge K edge; (ii) Ag foil; (iii) Ag$_2$S. The latter were run in transmission mode at the Ag K edge. A 15 mm Ag foil was placed directly in the beam to act as the Ag standard. The Ag$_2$S standard was run by grinding powdered Ag$_2$S with BN and placing the mixture in a sample holder with Be windows [8] which was then inserted into the beam. Background subtraction of the EXAFS spectra was carried out using the EXCALIB and EXBROOK programs available on the Daresbury Convex system. The spectra were fitted using the program EXCURV92 [9] also on the Daresbury Convex.
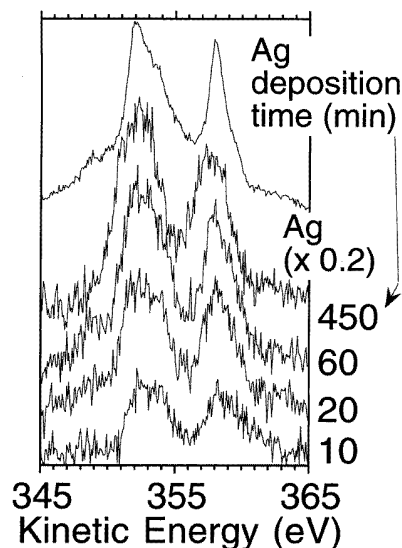
Figure 1. Ag M$_{4,5}$N$_{4,5}$N$_{4,5}$ XAES spectra as a function of Ag deposition time on GeS$_2$. The spectrum of clean Ag is also given for comparison.

3. Results and discussion

3.1. Ag deposition on clean GeS$_2$

By means of Auger spectroscopy, we have already shown that Ag grows on *clean* GeS$_2$ in a monolayer–simultaneous-monolayer (MSM) growth mode. The deposition of Ag on clean *and photo-oxidized* GeS$_2$ was investigated using XPS. No changes in Ag 3d$_{5/2}$ binding energy (367.9 eV) or peak shape were observed during Ag deposition. (The binding energy for thick Ag films deposited onto the Ni substrate was essentially the same—367.7 eV.) Figure 1 shows Ag M$_{4,5}$N$_{4,5}$N$_{4,5}$ XAES data as a function of Ag deposition time on an 80 Å clean GeS$_2$ film; the spectrum from clean Ag is also shown for comparison. It is apparent that the Ag XAE spectrum also undergoes little change with increasing deposition time, other than increased intensity, even at high coverages. However, in contrast to the Ag binding energy which remains unchanged, there are considerable differences when the XAES spectra are compared with that acquired for pure Ag metal. First, the spectra for Ag

deposited on GeS$_2$ lie at lower kinetic energies (E_k): the sharper $M_4N_{4,5}N_{4,5}$ contribution lies at 356.8 eV while that for metallic Ag is 358.0 eV. The resultant Auger parameters (α) are thus 724.7 eV and 725.7 eV respectively. The $M_4N_{4,5}N_{4,5}$ emission is also broader in the case of Ag deposited on GeS$_2$: a full width at half-maximum of 3.4 eV compared to 2.4 eV for metallic Ag. Finally, the intensities of both the Ag XAES and XPS signals from thick Ag deposits on GeS$_2$ are sharply reduced compared to those exhibited by metallic Ag. For example, after a deposition time of 450 min ($\sim$30 monolayers), the XAES peak is only about a fifth as intense as that from clean Ag, with the $3d_{5/2}$ peak a third as intense.
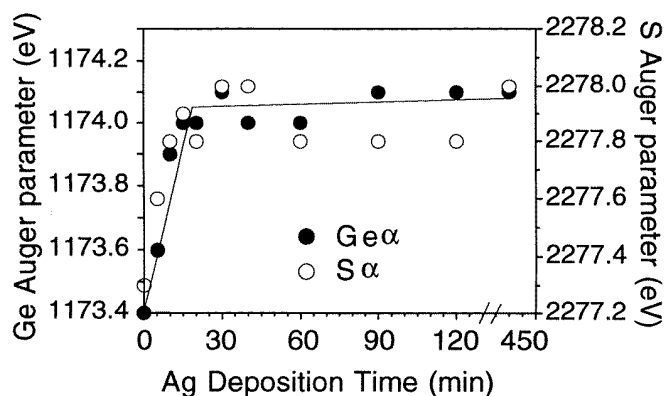

Figure 2. S and Ge Auger parameters as a function of Ag deposition time on GeS$_2$.

These results are consistent with chemical compound formation at the Ag/GeS$_2$ interface. The Auger parameter for Ag deposited on GeS$_2$ is similar to that for Ag$_2$S (724.8 eV [10]) and substantially different from that observed here and reported in the literature (726.0 eV [10, 11]) for pure metallic Ag. This demonstrates that on GeS$_2$ the deposited Ag has a considerable amount of sulphide character. The wide XAES peak observed suggests that several distinct Ag species exist in the interfacial contact region corresponding to differing degrees of sulphide or metallic character. The reduced peak intensities in the Ag XPS and XAES spectra are consistent with our previous observations on the electron-excited Auger emission during Ag deposition. There, the reduction in intensity was attributed to formation of an undefined Ag–S–Ge compound at the surface, reducing the number density of Ag atoms from that observed in the metal. Since the Ag peak intensity is still relatively weak even after a deposition time of 450 min, the thickness of the reacted layer must be significant, of the order of 30 monolayers, implying that the metal has diffused through much of the original GeS$_2$ layer. The S $2p_{1/2,3/2}$ and Ge $3d_{3/2,5/2}$ peak intensities are also consistent with this interpretation, having been attenuated to 30% and 50% respectively of their initial intensity after a deposition time of 450 min.

The Ge and S XP spectra also demonstrate the formation of an extensively reacted layer of GeS$_2$. Figure 2 shows the Ge and S Auger parameters as a function of Ag deposition time. As can be seen, the shift takes place over the first 20 min of Ag deposition, the time taken to reach the break point in the Auger uptake curve. The final value for α(Ge) is 1174.1 eV and that for α(S) is 2277.9 eV. The corresponding values for clean GeS$_2$ are 1173.1 eV and 2277.3 eV respectively. In the case of S, the $2p_{1/2,3/2}$ XPS binding energy (BE) shifts from 161.5 eV (GeS$_2$) to 161.3 eV. The S Auger parameter and BE shifts are consistent with both an increase in extra-atomic polarizability and reduction in

electronegativity of the S environment [12] which would be expected for the introduction of a metal into the lattice. However, the values are still different from those previously observed for bulk Ag_2S (BE = 159.6 eV and α = 2279.8 eV [10]). This demonstrates that while S does bond to Ag at the interface, there must still be a considerable degree of interaction with Ge, suggesting that S bridges Ge and Ag atoms in the lattice by forming Ag–S–Ge-type structures. The Ag-induced Ge chemical shift is from BE = 30.5 eV (GeS_2) to 29.8 eV. This, and the Auger parameter shift are consistent with the presence of metallic character in the Ge environment, possibly implying direct Ag–Ge bonding. However, the Auger parameter of 1174.1 eV is close to that observed for elemental Ge of 1174.4 eV, implying that formation of Ge–Ge bonds is also possible.

These observations are in general agreement with a previously proposed mechanism for the photodiffusion reaction of Ag in GeS_2 [2] according to which Ag initially reacts by breaking a S–Ge bond in the GeS_2 lattice

$$Ag^0 + S_3Ge–S–GeS_3 \rightarrow S_3Ge–S–Ag + \cdot GeS_3. \tag{1}$$
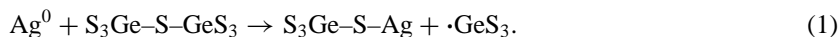
This results in bridging S atoms between Ge and Ag, as suggested by the S chemical shifts. It also leads to the formation of a Ag_2S-like environment for the Ag atoms. Furthermore, the $\cdot GeS_3$ unit should react with a neighbouring unit forming a Ge–Ge bond thus accounting for the observed shifts in Ge Auger parameter. Notice that this mechanism specifically precludes the formation of a direct Ag–Ge bond:

$$2GeS_3 \rightarrow S_3Ge–GeS_3. \tag{2}$$

On the basis of the XPS results alone however, we cannot rule out the possibility of first-shell Ag–Ge bonding in the interfacial compound.
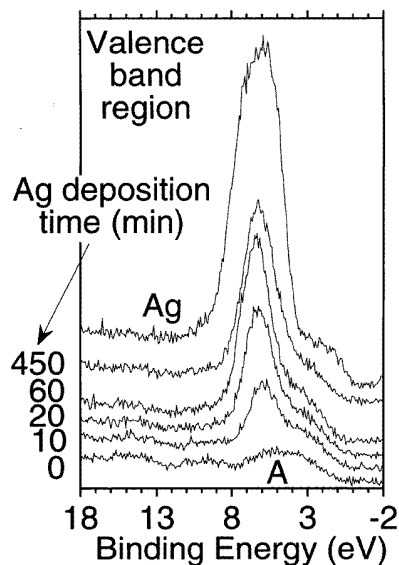

Figure 3. Valence band XP spectra as a function of Ag deposition time on GeS₂.

The present results are in striking contrast to those observed when Zn is deposited on GeS_2 [4]. In this latter case there was a clear distinction between the interfacial contact layer compound and overlying metallic Zn. Most importantly, the abrupt Zn/GeS_2 interface showed no evidence for Zn–S bond formation: only Zn–Ge bonding occurred in the contact layer region. These differences in behaviour between Ag and Zn are consistent with the

observation that whereas Ag photodiffusion in GeS_2 (and other ChVS) is quite facile, Zn photodiffusion is considerably less so [1]. The formation of a S-depleted interfacial layer in the Zn/GeS_2 system might also act as a blocking layer for further diffusion of the metal. In contrast, the extensive reacted layer formed in the case of Ag (where the metal occupies a number of different types of site) may permit facile photo-induced diffusion of the metal into the bulk.

Finally, we note that the valence band XP spectra (figure 3) are also consistent with the above interpretation of the XP core-level and XAE spectra. The principal Ag-derived density of states is the d band centred at a BE of about 5.5 eV. As can be seen in figure 3, the d-band contour is different for Ag metal and Ag deposited on GeS_2, suggesting the presence of a Ag compound whose valence electron density is unlike that of metallic Ag. In particular the line shape in the vicinity of the Fermi edge is characteristic of a semiconductor rather than a metal. Consistent with this, note that the FWHM of the Ag metal valence band is significantly greater than that of Ag/GeS_2 in line with the shorter photohole lifetime expected for a metal. The peaks in the GeS_2 spectrum at energies above 8 eV attributable to Ge and S s states are rapidly attenuated by the presence of Ag, demonstrating that changes also occur in the electronic structure of the ChVS. The Ag d bands are found in the region of the GeS_2 valence band which contains Ge 4p–S 3p bonding states [13]. Thus Ag d electrons lie at the correct energy for electron donation into the Ge–S bond, as required in the mechanism outlined by reactions (1) and (2). In the present case, comparison of the XP spectral intensities from the pure Ag sample and from the 450 min film shows that this ratio is considerably lower than the corresponding value of 5 which is observed in the case of the Ag MNN XAE spectra (figure 1). Given the different electron kinetic energies and sampling depths in the two cases, this provides qualitative confirmation that Ag diffusion into GeS_2 has occurred.
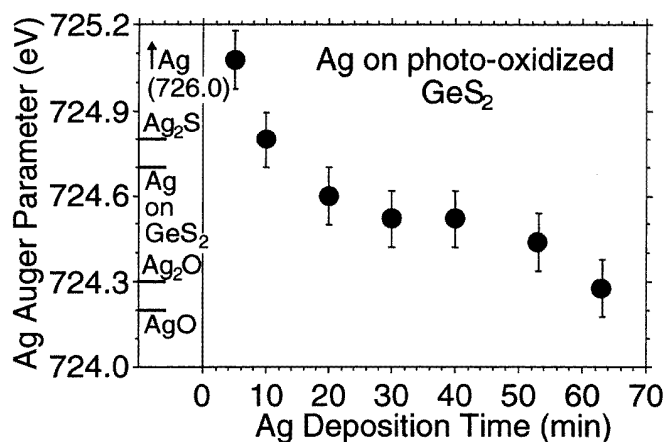

**Figure 4.** The Ag Auger parameter as a function of Ag deposition time on photo-oxidized GeS_2.

3.2. Ag deposition on photo-oxidized GeS_2

Figure 4 shows the Ag Auger parameter as a function of deposition time upon a photo-oxidized GeS_2 film; unlike in the case of clean GeS_2, here the Ag Auger parameter varies considerably over the deposition period. It starts at a value of 725.1 eV at a deposition

time of 5 min, falling to 724.6 eV, typical of that previously observed for Ag deposition on clean GeS_2. This suggests that the Ag initially deposited on the photo-oxidized surface has less sulphide character than that deposited on the clean film, and thus that the presence of O on the surface tends to inhibit the reaction between GeS_2 and Ag. However, by the time the monolayer point is reached, the Ag Auger parameter has taken on a value characteristic of Ag_2S and of the Ag compound formed when Ag is deposited on clean GeS_2. For longer deposition times (50–60 min) the Auger parameter falls to 724.3–724.4 eV, which is more typical of the silver oxides (AgO, 724.2 eV; Ag_2O, 724.3 eV [10]). Thus initially, Ag deposited on the photo-oxidized surface exhibits more metallic character than on the clean GeS_2 film. However, the XP data show that by the time one layer of metal has been deposited, there appears to be little difference in the electronic properties of the Ag atoms between the two cases. The Ag $M_{4,5}N_{4,5}N_{4,5}$ Auger data indicate Stranski–Krastanov growth of Ag on photo-oxidized GeS_2, in agreement with earlier work [5]. These observations demonstrate that while initially the overlying Ag structures are metallic in character, the contact layer Ag continues to react with the photo-oxidized GeS_2 substrate. Eventually, the Ag islands must become large enough that Ag begins to interact significantly with O atoms on the GeS_2 surface, leading to the lowered value of α observed for longer deposition times.
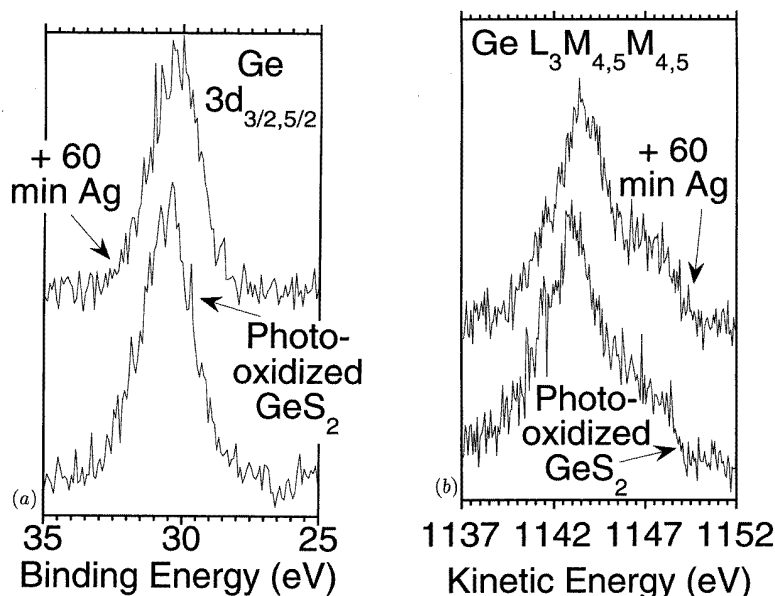
Figure 5. (a) Ge 3d XPS and (b) $L_3M_{4,5}M_{4,5}$ XAE spectra as a functions of Ag deposition time on photo-oxidized GeS_2.

Unlike in the case of Ag deposition on clean GeS_2, the Ge XP spectra indicate little or no initial reaction between Ge sites and the deposited Ag. The Ge XPS and XAES data (figure 5) show no attenuation and no spectral changes after sixty minutes of Ag deposition. In marked contrast, the S XP and XAE spectra exhibit essentially the same chemical shift behaviour as was observed on the clean film, clearly demonstrating that Ag continues to react with the (non-oxidized) S sites at the surface. We are therefore in a position to understand the very large differences in uptake behaviour exhibited by Ag and Zn on the photo-oxidized GeS_2 surface. In both cases, photo-oxidation of the Ge sites inhibits metal sticking at these
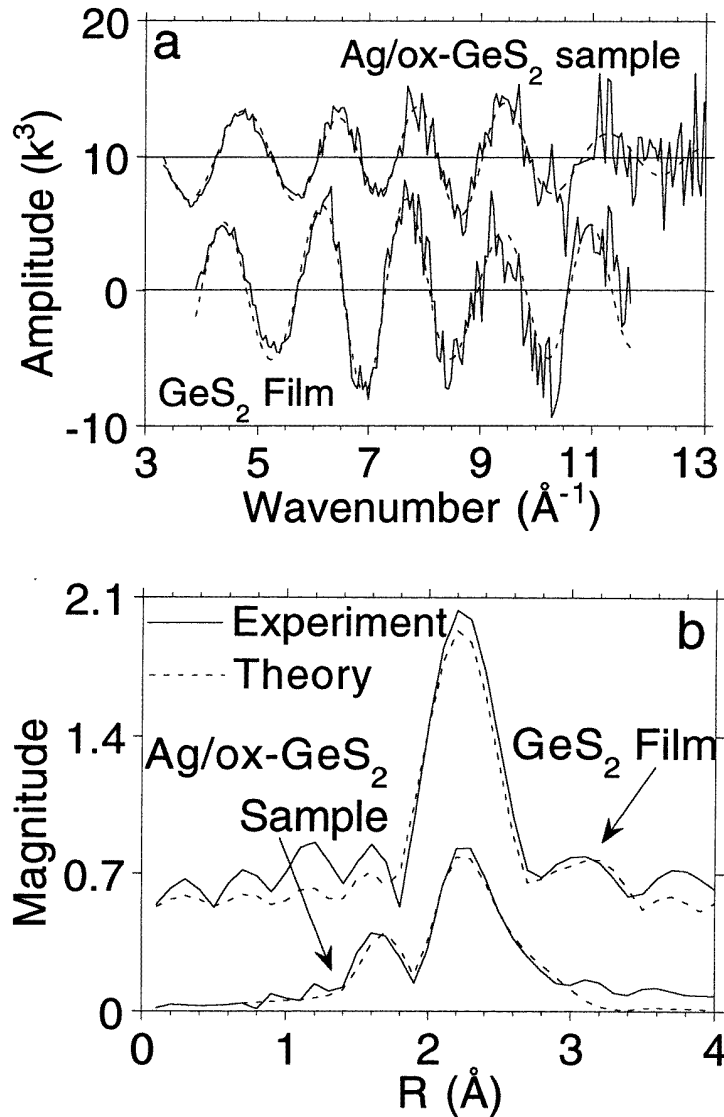
Figure 6. The Ge K-edge k^3 EXAFS in units of Å^{-3} (a) and the Fourier transform in units of Å^3 (b) for a clean GeS_2 film and sample 2.

sites. *However, Ag sticks, reacts and grows at the unoxidized S sites, whereas Zn cannot.* The dramatic change in sticking probability induced by photo-oxidation of GeS_2 which occurs in the case of Zn but not in the case of Ag is therefore explicable. While Ag exhibits no large changes in sticking probability, our results indicate that at the Ag/photo-oxidized GeS_2 interface there are regions of ChVS which have not reacted with the metal. These regions might act as a barrier to Ag photodiffusion into the bulk of the substrate, thus explaining induction periods of low diffusion rate that can occur in the early stages of photodiffusion. Such induction periods have indeed been ascribed to the formation of a blocking layer of some description [14, 15] and the present study establishes the actual presence of such a

barrier, around or through which diffusion must occur to give a continuous layer of reaction product. Our results also demonstrate that sample cleanliness might well be an important factor in this effect, since the oxidized ChVS surface gives rise to a much less homogeneous metal/ChVS interface as compared to the clean semiconductor film.

Table 1. EXAFS parameters for the Ge K-edge spectra.

Parameter		80 Å GeS$_2$ film	Ag/ox-GeS$_2$ sample
First shell (Ge–O)	R1 (Å)	N/A	1.757 ± 0.005
	N1		0.004 ± 0.001
	A1 (Å^2)		1.18 ± 0.06
Second shell (Ge–O)	R2 (Å)	2.261 ± 0.002	2.261 ± 0.004
	N2	3.7 ± 0.1	0.007 ± 0.001
	A2 (Å^2)	0.0063 ± 0.0006	1.59 ± 0.08
Third shell (Ge–Ge)	R3 (Å)	2.95 ± 0.01	2.43 ± 0.02
	N3	2.4 ± 0.5	2.7 ± 0.2
	A3 (Å^2)	0.021 ± 0.003	0.023 ± 0.005
E_F (eV)		-8.7 ± 0.3	-6.4 ± 0.2
AFAC		0.7 ± 0.2	0.7 ± 0.3
R-factor		39.7	30.36

Table 2. EXAFS parameters for the Ag K-edge spectra (figure 7).

Parameter		Sample 2 Ag/GeS$_2$	Sample 3 Ag/ox-GeS$_2$	Ag foil	Ag$_2$S
Shell 1 Ag–S	R1 (Å)	2.53 ± 0.03	2.54 ± 0.04	N/A	2.511 ± 0.005
	A1 (Å^2)	0.023 ± 0.008	0.032 ± 0.001		0.021 ± 0.001
	N1	0.8 ± 0.3	1.3 ± 0.6		2.5
Shell 2 Ag–Ag	R2	2.859 ± 0.002	2.86 ± 0.005	2.864 ± 0.001	2.91 ± 0.02
	A2	0.0169 ± 0.0006	0.021 ± 0.001	0.0189 ± 0.0004	0.047 ± 0.005
	N2	9.5 ± 0.3	7.3 ± 0.5 12	4.5	
Shell 3 Ag–Ag	R3	2.99 ± 0.03	2.99 ± 0.03	4.015 ± 0.009	3.09 ± 0.04
	A3	0.020 ± 0.003	0.030 ± 0.008	0.027 ± 0.002	0.05 ± 0.01
	N3	2.6 ± 0.4	2.5 ± 1.0	6	2.5
Ag–Ag	R4	N/A	N/A	4.965 ± 0.008	N/A
	A4			0.033 ± 0.002	
	N4			24	
Ag–Ag	R5	N/A	N/A	5.60 ± 0.01	N/A
	A5			0.025 ± 0.003	
	N5			12	
Ag–Ag	R6	N/A	N/A	6.04 ± 0.04	N/A
	A6			0.05 ± 0.01	
	N6			24	
AFAC		0.82 ± 0.02	0.86 ± 0.06	0.91 ± 0.03	0.78 ± 0.05
E_F		3.4 ± 0.2	1.6 ± 0.6	0.5 ± 0.3	1.8 ± 0.6
R-factor		46.3	54.3	20.4	34.5
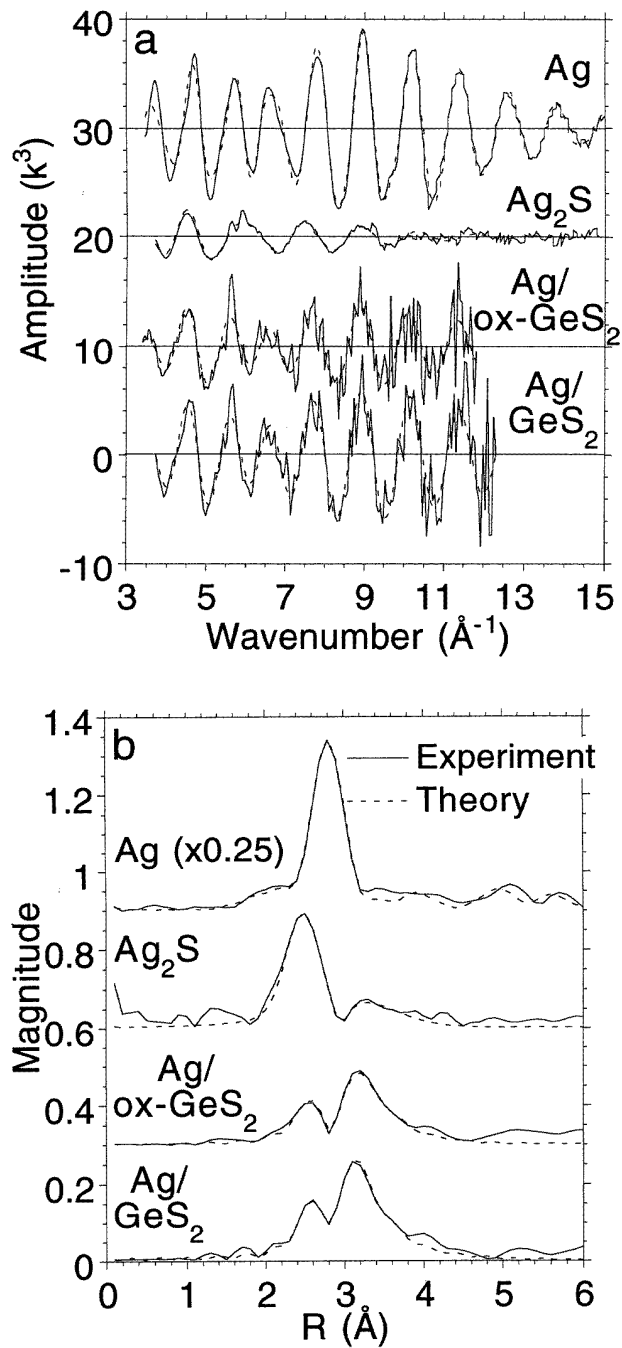
Figure 7. The Ag K-edge k^3 EXAFS in units of Å^{-3} (a) and the Fourier transform in units of Å^3 (b) for a Ag foil, Ag_2S and samples 1 and 2.

4. EXAFS

The Ge K-edge EXAFS and corresponding Fourier transform for an 80 Å GeS_2 film and for (photo-oxidized) sample 2 are shown in figure 6; associated fitting parameters

are given in table 1. A Ge K-edge spectrum was also acquired for (unoxidized) sample 1, the Ag/GeS$_2$ sample, but this spectrum was dominated by peaks attributable to Ge–Ni alloy formation. This was due to contamination of the Ni substrate by GeS$_2$ which had diffused into the substrate over the course of previous experiments. Both the GeS$_2$ film standard and sample 2 were prepared on a new substrate, and this problem was not encountered. The GeS$_2$ film EXAFS spectrum indicates the presence of two shells, both of the corresponding bond lengths being typical of the high-temperature α form of crystalline GeS$_2$ [16], demonstrating the similarity of this amorphous film to the crystalline material in the first two coordination shells. The first-shell Ge–S bond length at 2.27 Å is also seen in the EXAFS spectrum of sample 2, as expected, although here the coordination number is considerably reduced from the ideal value of 4. Clearly the presence of Ag leads to disruption of Ge–S bonds. A Ge–Ge shell is also seen in both spectra, but the bond distance is very different in the two cases: 2.95 Å for the GeS$_2$ film and 2.43 Å for the photo-oxidized sample 2. In the GeS$_2$ film the Ge–Ge distance corresponds to the second coordination shell, i.e. between two Ge atoms in edge-sharing GeS$_4$ tetrahedra [16–18] of glassy GeS$_2$. However, the Ge–Ge bond distance of 2.43 Å observed for sample 2 is typical of elemental Ge (2.45 Å [19]). This strongly suggests formation of homopolar Ge–Ge bonds when Ag is deposited on GeS$_2$, and, given the absence of the Ge–Ge distance at 2.95 Å in the sample 2 spectrum, break-up of the network of interconnected chains of GeS$_4$ tetrahedra in the glass. Such an interpretation is in agreement with the mechanism for Ag photodiffusion outlined in the previous section. Finally, the spectrum of sample 2 indicated a Ge–O bond distance typical of the high-temperature form of GeO$_2$ [20], arising from the photo-oxidation treatment, in good accordance with our photoemission results. The Ag K-edge EXAFS spectra and corresponding Fourier transforms for the Ag foil, Ag$_2$S standard, sample 1 and sample 2 are shown in figure 7; associated fitting parameters are given in table 2. These are fairly straightforward to interpret. An examination of the results indicates that bond distances typical of both Ag and Ag$_2$S contribute to the overall sample spectra. Thus, when deposited on GeS$_2$, Ag appears to react partially with the ChVS substrate forming a Ag$_2$S-like compound. This is in agreement with previous work on GeSe$_2$ films photodoped with Ag and in Ag–Ge–S and Ag–As–S glasses [17, 21] and with our photoemission data. However, the presence of Ag–Ag distances typical of metallic Ag demonstrates that, as suggested by the XP spectra, the reaction between GeS$_2$ and Ag is not complete, and that considerable amounts of unreacted Ag remain at the interface. This is quite different to the results of previous work mentioned above: in these cases no evidence for unreacted metallic Ag was found [17, 21] which is presumably a consequence of the complete photo-induced diffusion of Ag into the substrate. In our case, Ag is merely deposited on the surface and any diffusion into the bulk is thermally induced; not unexpectedly the extent of the reaction is not as great as in the photodiffusion case.

Finally, we note that both the Ag and Ge K-edge spectra show no evidence for direct Ge–Ag bonding at the interface. This is also in agreement with EXAFS of Ag–ChVS systems in which only direct silver–chalcogen bonds are observed [17, 21]. This demonstrates that the chemical shifts observed for Ge in the XPS data must be due to homopolar Ge–Ge bond formation and not Ag–Ge bonds.

5. Conclusions

1. Ag grows on clean GeS$_2$ in the MSM growth mode reacting extensively with the GeS$_2$ substrate and resulting in modification of the electronic properties of all three elements. The Auger parameter and chemical shift data demonstrate the formation of Ag–S bonds in

the interfacial region, suggesting formation of Ag–S–Ge structures. These observations are consistent with previous mechanisms proposed for the photodiffusion reaction, as are the valence band XPS data.

2. On the photo-oxidized film, Ag grows in a Stranski–Krastanov mode with the overlying Ag islands continuing to react extensively to form silver sulphides. There is little interaction between Ag and the oxidized Ge sites on the surface, although silver oxides are formed at high coverages.

3. EXAFS spectra at the Ag K edge of layered Ag/GeS_2 samples indicate the presence of Ag–S and Ag–Ag coordination at the interface typical of Ag_2S. However, considerable amounts of metallic Ag persist. The Ge K-edge spectra indicate that Ag tends to break up the chains of GeS_4 tetrahedra present in the amorphous film, and brings about the formation of homopolar Ge–Ge bonding. In agreement with previous work on bulk systems, there is no evidence for direct Ag–Ge bond formation at the interface.

4. Proposed models for the photodiffusion mechanism, and the phenomenon of induction periods during the photodiffusion reaction can be rationalized using these results. There are also large differences between these results and those obtained for Zn deposition on GeS_2, which explain the origin of the unusual sticking probability phenomena observed with Zn, but not with Ag.

Acknowledgments

References

[1] Kolobov A V and Elliott S R 1991 *Adv. Phys.* **40** 625
[2] Elliott S R 1991 *J. Non-Cryst. Solids* **130** 85
[3] Bedel'baeva G B, Kolobov A V and Lyubin V M 1989 *Phil. Mag.* B **60** 689
[4] Horton J H, Hardacre C, Baddeley C J, Moggridge G D, Ormerod R M and Lambert R M 1995 *Phys. Rev.* B **52** 2054
[5] Horton J H, Peat K L and Lambert R M 1993 *J. Phys.: Condens. Matter* **5** 9037
[6] Horton J H, Moggridge G D, Ormerod R M, Kolobov A V and Lambert R M 1994 *Thin Solid Films* **237** 134
[7] Hardacre C, Ormerod R M and Lambert R M 1993 *Chem. Phys. Lett.* **206** 171
[8] Koningsberger D C (ed) 1988 *X-Ray Absorption* (New York: Wiley)
[9] Binsted N, Campbell J W, Gurman S J and Stephenson P C 1991 *EXCURV92 Program* SERC Daresbury Laboratory
[10] Kaushik V K 1991 *J. Electron Spectrosc. Relat. Phenom.* **56** 273
[11] Briggs D and Seah M P (ed) 1990 *Auger and X-Ray Photoelectron Spectroscopy (Practical Surface Analysis 1)* 2nd edn (Chichester: Wiley)
[12] Wagner C D 1975 *Faraday Discuss. Chem. Soc.* **60** 291
[13] Takahashi T, Haradu Y and Hino S 1979 *Solid State Commun.* **30** 635
[14] Chatani K, Shimizu I, Kokada H and Inoue E 1977 *Japan. J. Appl. Phys.* **16** 389
[15] Wagner T and Frumar M 1990 *J. Non-Cryst. Solids* **90** 489
[16] Dittmar V G and Schaefer H 1975 *Acta Crystallogr.* B **31** 5452
[17] Armand P, Ibanez A, Dexpert H and Philippot E 1992 *J. Non-Cryst. Solids* **139** 137
[18] Elliott S R 1990 *Physics of Amorphous Materials* 2nd edn (Harlow: Longman Scientific & Technical)
[19] Kittel C 1986 *Introduction to Solid State Physics* 6th edn (New York: Wiley)
[20] Lee J H, Owens A P and Elliott S R 1993 *J. Non-Cryst. Solids* **166** 139
[21] Steel A T, Greaves G N, Firth A P and Owen A E 1989 *J. Non-Cryst. Solids* **107** 155